Chapter 3

Modified Spin Coating Method for Coating and Fabricating Ferroelectric Thin Films as Sensors and Solar Cells

Irzaman, Heriyanto Syafutra, Ridwan Siskandar, Aminullah and Husin Alatas

Additional information is available at the end of the chapter

http://dx.doi.org/10.5772/66815

Abstract

Spin coating process with a modified spin coater is performed well, especially the second generation of modified spin coater, which has a maximum value of 18,000 rpm, is able for manufacturing/coating photonic crystal-based ferroelectric thin films that require a high angular velocity (rpm). Ferroelectric thin films that use both 3000 and 6000 rpm have given good results in energy gap, electrical conductivity, etc. In addition, the modified spin coater has also produced several applications such as sensors in the device of blood sugar level noninvasively, sensors in the automatic drying system, sensors in the robotic system, and photovoltaic cells in the system of solar cells/panels which are being developed at present. These applications used ferroelectric material such as barium strontium titanate (BST), lithium niobate ($LiNbO_3$), cuprous oxide (CuO), and lithium tantalate ($LiTaO_3$).

Keywords: modified spin coating, ferroelectric thin films, sensors, solar cells

1. Introduction

Thin film technology is one of the pillars of the current smart material technology due to its material and cost efficiencies. Industrial applications of thin films include electronic semiconductors (especially solar cells), optical coatings, and sensors due to their dielectric constant, dielectric loss, pyroelectric coefficient, and dielectric tunability properties. Ferroelectric thin films such as barium strontium titanate, lithium tantalate, and lithium niobate can be manufactured by using CSD method and then performed by the spin coating process [1]. CSD method is one of the methods to create/develop thin films [2–12], which has advantages including the ability to control the film stoichiometry with good quality, easy procedure,

require relatively low cost, and generate a good crystalline phase [13–15]. In addition, thin films can also be fabricated by other methods such as metal organic chemical vapor deposition (MOCVD) [16–18], chemical vapor deposition [19], sol-gel [20–23], atomic layer deposition (ALD) [24], metal organic decomposition (MOD) [25], pulsed laser ablation deposition (PLAD) [26, 27], and RF sputtering [2, 21, 28].

Spin coating is a method for coating and fabricating uniform thin films by rotating substrate and solution of thin films with a certain angular velocity. Purwanto and Prajitno [29] stated that spin coating is a method to deposit a thin film by spreading the solution onto a substrate by utilizing the centripetal force, the substrate is rotated at a constant velocity and then thin film precipitate is obtained on the substrate. Spin coating process has several advantages: namely, it is a simple method that can be done at room temperature, and low cost, yet effective enough for manufacturing thin films [30]. Coating technique with spin coating method is the best technique used to produce thin films with uniform thickness ranging from 0.3 to 5.0 μm on the substrate surfaces that are relatively small [31, 32]. The film thickness is determined by the flow rate and plating time [33]. A simple process of spin coating can be seen in **Figure 1**.

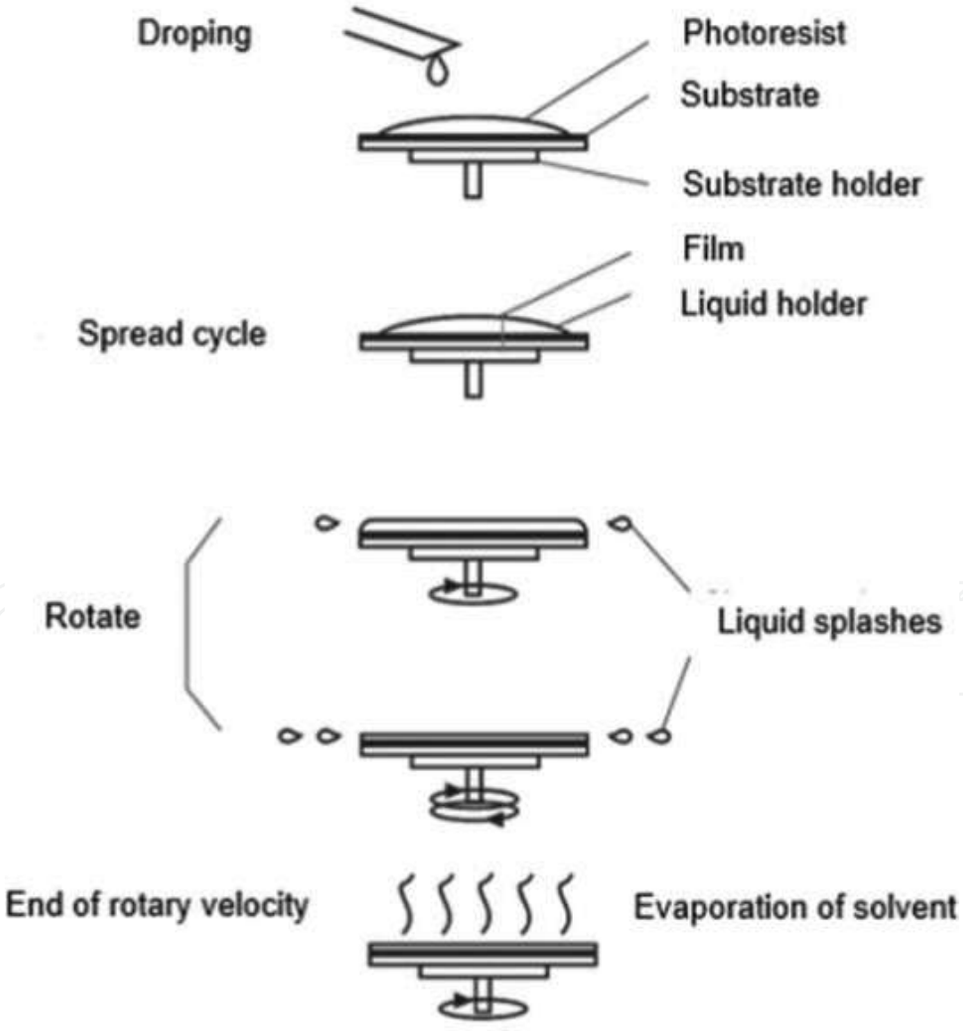

Figure 1. Simple process of spin coating [20, 21].

http://dx.doi.org/10.5772/66815

2. First generation of modified spin coater

Proper design of the modified spin coating can reduce cost in the international market because its components can be purchased in Indonesia and adequate for our laboratory-scale research. A schematic design of portable spin coating type 2004 can be seen in **Figure 2**. This device can be carried easily because it is very light and small as well as better than the traditional one in operational and production costs as well as in efficiency. For generating or rotating the disk in a spin coating, the step-down transformer of 1 A is required with the output voltages based on the digital system. The output voltages of 7, 9, and 12 V are connected to the potentiometer, diode, and capacitor which resulting in the spin coating rotation of 3480, 4380, and 5840 rpms, respectively. The accuration test of the rotational velocity can be conducted by using a stroboscope.

The work mechanism of the device is as follows: the solution of thin films is dripped on a substrate which has been placed on the spin coating device. Then, the attached solution on a substrate is rotated at the desired rpm velocity. The voltage source used in the device is 220 V AC with current of 1 A, which is obtained through the step-down transformer. The output voltage of 7, 9 or 12 V can be selected via potentiometer setting. A diode serves to rectify the AC current into DC and then the electrical charges stored in a capacitor. The rotations are about 3480, 4380, and 5840 rpms.

The modified spin coating device (**Figure 2**), which its patent has been registered in Indonesia with a number of P00201201122 in 2013, has a structural design that consists of four components.

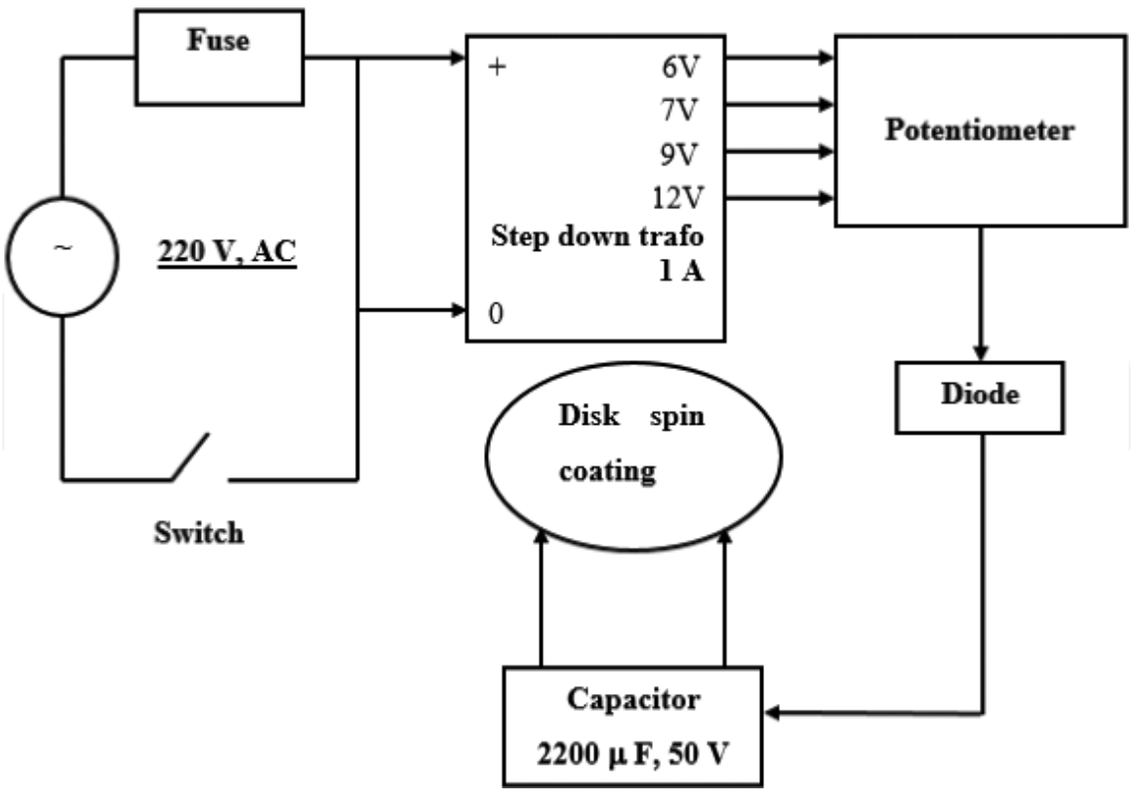

Figure 2. Design of portable spin coating-type 2004.

2.1. Current source

A current source of 220 V AC is connected to the switch and fuse safety systems.

2.2. Step-down transformer and potentiometer

A step-down transformer of 1A with input voltages of 7, 9 and 12 V. These are a set based on the resistance that changes in the potentiometer.

2.3. Diode and capacitor

A rectifier diode of standard currents is used to deliver a DC current of 50 V into a capacitor of 2200 μF and 50 V. The capacitor serves to store the charges and acts as a charge source for powering the disk spinner.

2.4. Disk of spin coating

The aluminum spinner device with a radius of 4 cm and thickness of 0.2 cm is used to rotate the substrate that has been dripped by solution of thin films. To generate rotation, a rotator machine is used to achieve the desired rpm velocity. **Figure 3** shows the exterior of the modified spin coating device. A disk spinner installed on a plastic container of PVC with a radius of 6 cm and thickness of 0.3 cm and a steel cantilever with a thickness of 2 cm and an area of 4 cm × 4 cm to stabilize the disk spinner. The electrical circuits are arranged in a container of 6.2 cm × 19 cm.

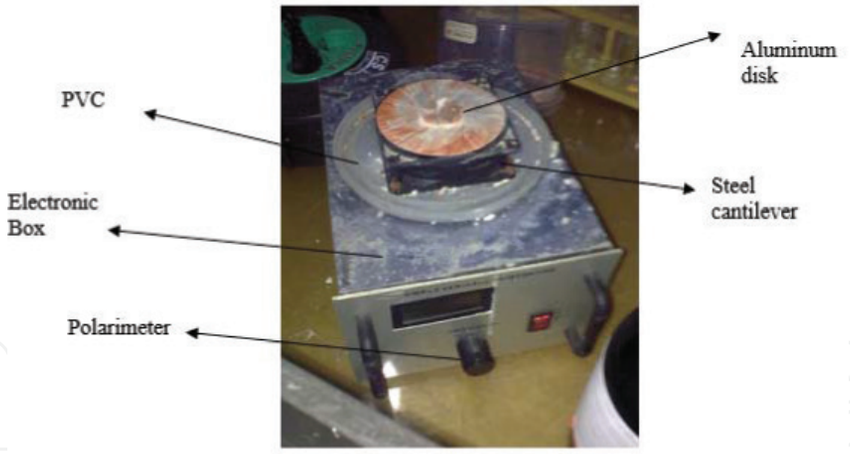

Figure 3. Exterior of the modified spin coating device.

3. Second generation of the modified spin coater

Currently, the development of the spin coating device has started in which the angular velocity of the device is increased up to 18,000 rpm. This is done because the manufacture of ferroelectric-based photonic crystals thin films requires a high-angular velocity. There are five stages in the development of a high-velocity spin coating device, namely designing, manufacturing, testing, analyzing, and developing the device.

http://dx.doi.org/10.5772/66815

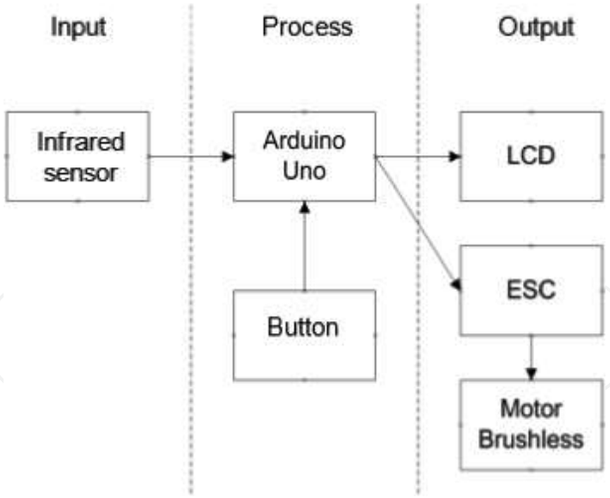

Figure 4. Block diagram.

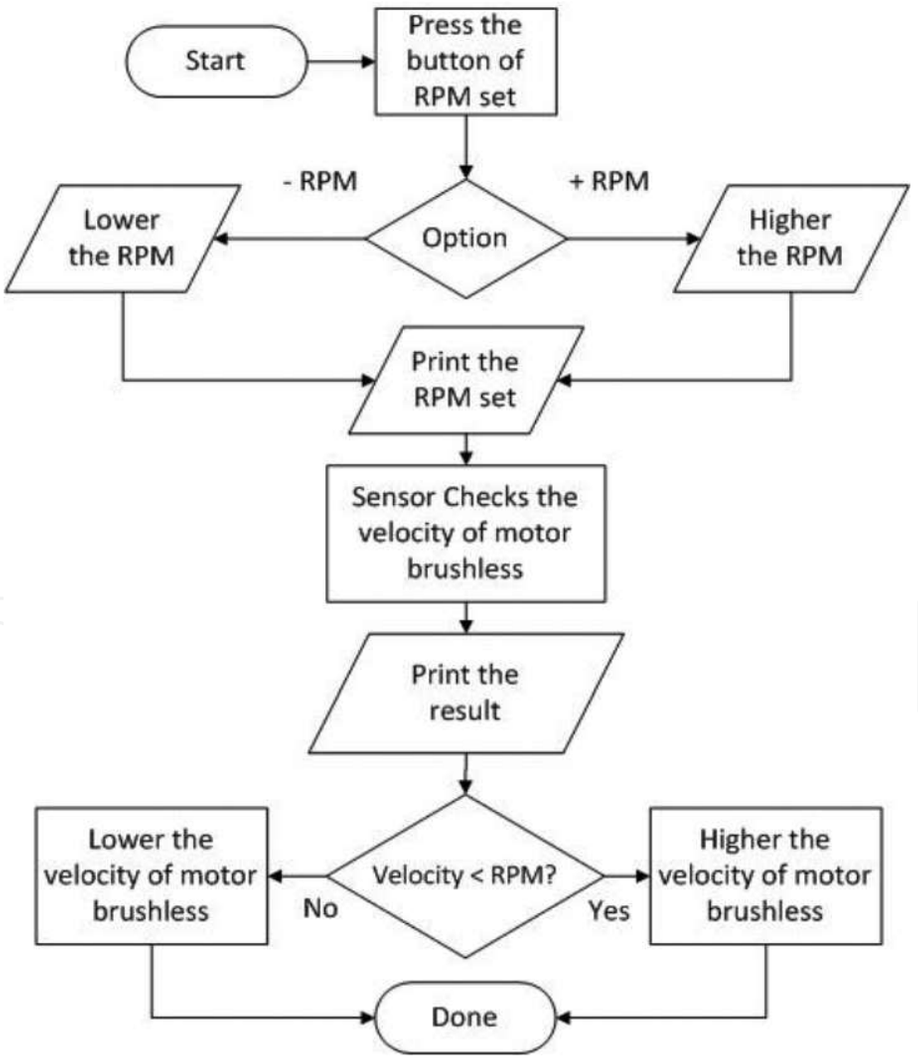

Figure 5. Program flowchart.

3.1. Designing the device

In this stage, designing the workflow is conducted which is described in the block diagram and flowchart. The block diagram in **Figure 4** illustrates the Arduino Uno as a data processing center that received input from infrared sensors, controlled by the buttons, and the output as a signal to adjust the angular velocity of a brushless motor as the driving component via the ESC motor driver and the LCD will show the magnitude of the angular velocity in rotation per minute (RPM). **Figure 5** shows the program flowchart for a device that further will be integrated with the Arduino Uno.

3.2. Manufacturing the device

The schematic circuit diagram in **Figure 6** describes the use of Arduino Uno, buttons, infrared sensor, ESC, brushless motor, and LCD. There are eight Arduino pins, six digital, and two analog pins, which are used for the data path. Pin 4–7 on Arduino connected to four buttons. In connecting the ESC to Arduino, pins that support the pulse width modulation (PWM) are needed, so pin 3 was used on the Arduino. Infrared sensors require attach interrupt function on the program of pin 2. Then, to connect Arduino to LCD, I2C interface used to conserve the use of pins on the Arduino. From the circuit scheme, A4 pin on the Arduino is connected to the SLC in the I2C interface and A5 pin on the Arduino is connected to the SDA in I2C interface. The brushless motor has only three wires and those are connected to the ESC.

The used voltage source is an adapter of 12 V and 5 A. Most of the voltage source used to drive a brushless motor and ESC by using a voltage of 12 V and current of 5 A. Arduino gets voltage from the same source, but also need a resistor of 20 Ω on V_{in} pin in order not to damage Arduino. While other components such as infrared sensors, I2C interface, and LCD can be run at a voltage of 5 V.

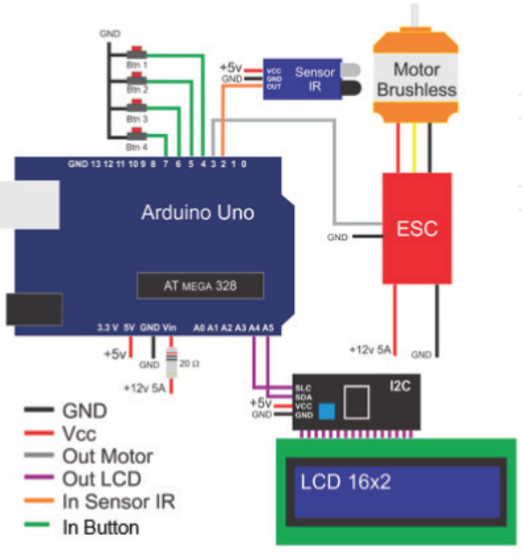

Figure 6. Circuit schematic.

http://dx.doi.org/10.5772/66815

After making a circuit scheme, the program code is conducted in accordance with the device workflow diagram that has been made at the designing stage. When the device circuit and the program code are completely made, it is necessary to merge the process of the device circuit with the program code so that the device can work in accordance with the flowchart. The incorporation using an application that matches to the Arduino device is Arduino IDE 1.6.8. Interface of Arduino IDE 1.6.8 application is shown in **Figure 7**.

3.3. Testing the device

LCD displays the measurement of angular velocity and value rpm. As can be seen from **Figure 8**, the first line of LCD includes the word "Speed" that shows the measurement of the angular velocity in units of rpm. The second line of LCD is"Set' that shows the rpm setting value that users want in units of rpm as well. **Table 1** shows the measured voltages and currents between circuit blocks of the spin coater which explains that an infrared sensor will produce an output voltage of 4.92 V if detects black color and will produce an output voltage of 0.11 Vif detects another colors. Arduino circuit blocks will produce different output voltage according to the type of the use of the IC.

The next is the accuracy of angular velocity of the spin coater using tachometer type DT-2234C^{+} as an angular velocity comparator (**Figure 9**). Angular velocities of the brushless motor are determined on the value from 1000 to 20,000 rpm.

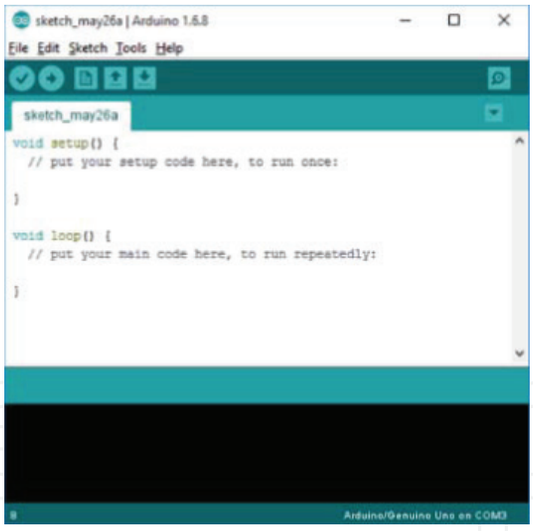

Figure 7. Interface of Arduino IDE 1.6.8.

Figure 8. Test result.

Circuit blocks	V_{in} **(V)**	V_{out} **(V)**	I **(mA)**
ESC	12.01	~	5000
Infrared sensor			
Detects black color	4.92	4.92	3.3
Detects another colors	4.92	0.11	3.3
Arduino			
Set of 0 rpm	11.07	0.21	0.11
Set of 4000 rpm	11.07	0.23	0.11
Set of 5000 rpm	11.07	0.24	0.11
Set of 6000 rpm	11.07	0.25	0.11
Set of 7000 rpm	11.07	0.25	0.11
Set of 8000 rpm	11.07	0.27	0.11
Set of 9000 rpm	11.07	0.28	0.11
Set of 10,000 rpm	11.07	0.29	0.11
Set of 11,000 rpm	11.07	0.3	0.11
Set of 12,000 rpm	11.07	0.33	0.11
Set of 13,000 rpm	11.07	0.35	0.11
Set of 14,000 rpm	11.07	0.41	0.11
Set of 15,000 rpm	11.07	0.51	0.11
Set of 16,000 rpm	11.07	0.53	0.11
Set of 17,000 rpm	11.07	0.58	0.11
Set of 18,000 rpm	11.07	0.6	0.11
LCD			
Pin *V*cc	4.91	–	3.3
Pin SDA	2.13	–	0.12
Pin SLC	2.58	–	0.01

Table 1. Measurements of voltage and current between circuit blocks.

From the experimental data, the brushless motor is only capable of producing the minimum angular velocity of 4000 rpm and the maximum of 18,000 rpm with no load. In addition, angular velocity on the spin coater has an average difference of 82.67 rpm obtained from the tachometer. The data can be seen in **Table 2** and **Figure 10**.

3.4. Development analysis

A function menu is added in the program of development. In this function, users can choose the mode of use, i.e., manual and automatic modes. In automatic mode, users need to set

http://dx.doi.org/10.5772/66815

Figure 9. Tachometer type DT-2234C+.

the number of repetitions (step), the length of timer (timer), and the angular velocity (rpm set). The number of repetitions is only for a substrate. When the timer is up it is necessary to notify such as a sound, hence the buzzer circuit is added as a component to produce a sound as shown in **Figure 11(a)**. In addition, a button is also added, as shown in **Figure 11(b)**, as a supporter of the functions that will be created. The added button is useful for stop the button when the spin coater is started. The development of block diagram shown in **Figure 12** is not much different from the block diagram of before device development.

3.5. Development

The development of schematic circuit designing and flow of program are conducted in this stage. The developed schematic circuit shown in **Figure 13** is not much different from previous schematic, only different in add buzzer and button components. A buzzer and a button are connected directly to the Arduino via pins 9 and 8, respectively. Overall device development and its power supply can be seen in **Figure 14**.

A flow diagram in **Figure 15** shows the flow of the program code. First, the user is prompted to select the mode to be used. The available modes are manual and automatic modes are shown in **Figure 16**. If users select the manual mode, it will display a condition before the device was developed. When choosing the automatic mode, the user is prompted to set the number

Angular velocity (rpm)		
Set value	**Spin coater (infrared sensor)**	**Tachometer**
4000	4200	4200
5000	5280	5285
6000	6360	6342
7000	7380	7406
8000	8340	8470
9000	9540	9541
10,000	10,500	10,504
11,000	11,460	11,406
12,000	12,360	12,442
13,000	13,560	13,621
14,000	14,220	14,428
15,000	15,240	15,408
16,000	16,200	16,367
17,000	17,280	17,521
18,000	18,060	18,135

Table 2. The comparison results of angular velocity.

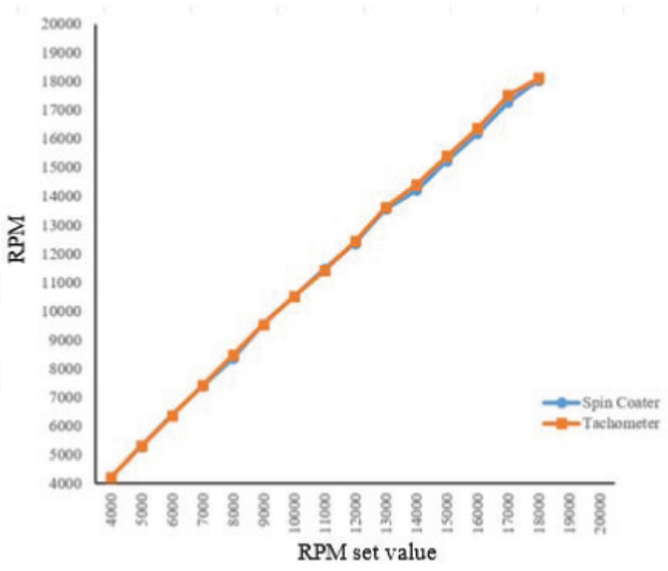

Figure 10. Angular velocity comparison.

of repetitions as shown in **Figure 17**, then adjust the angular velocity in rpm as shown in **Figure 18**, and set the length of time in seconds as shown in **Figure 19**. Once the setup process is complete, it will display a summary which is shown in **Figure 20** and then confirm to save the setting on Electrical Erasable Programmable Read-only Memory (EEPROM) on Arduino

http://dx.doi.org/10.5772/66815

Figure 11. Buzzer (a) and button (b) component.

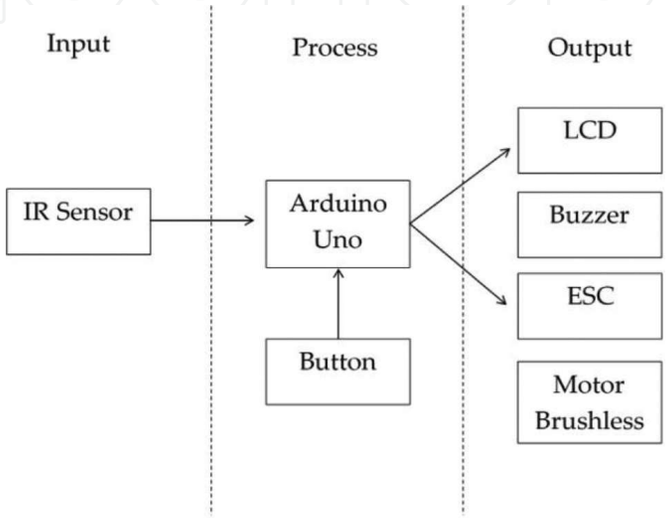

Figure 12. Development diagram.

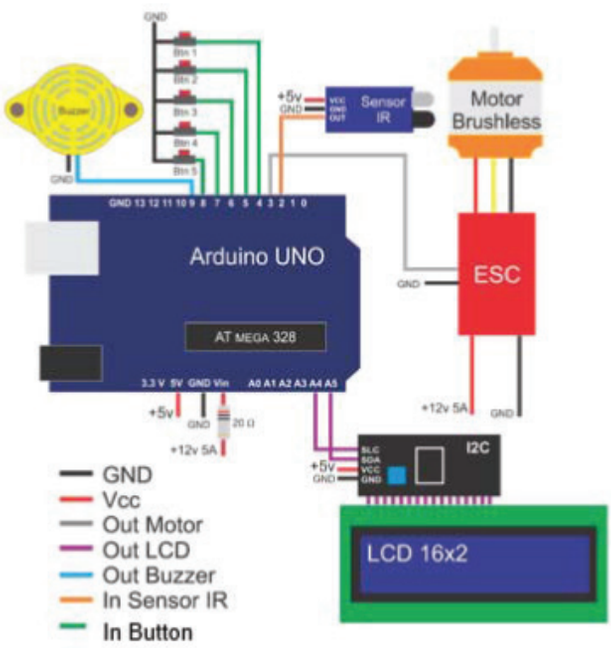

Figure 13. Development circuit schematic.

Figure 14. Overall device development and its power supply.

semipermanently which is not lost when the power supply is not connected as in **Figure 21**. The save settings will display words of"Saving Data" as shown in **Figure 22**, after the save process is completed it will display the words of"Data saved" as shown in **Figure 23** and **a** buzzer will sound twice. If not saved then it will return to the setup process.

Once the data has been stored, the spin coater will begin the process of spin coating which displays some information such as repetition, duration, time remaining on the first line of the LCD, and the rpm setting value and measurement results of angular velocity on the second line of the LCD as in **Figure 24**. At each repetition process, the buzzer will sound once. If the spin coating process has been completed, it will display word of"Done" as shown in **Figure 25** and **a** buzzer will sound three times, after that confirmation of the spin coating reprocess will be also displayed as in **Figure 26**.

The aim of this stage is to improve the device accuracy by conducting device reconfiguration. The device reconfiguration will change the measurement of angular velocity, then retest must be done for the accuracy of device. The testing method as well as the testing method before development is compared to tachometer-type DT-2234C+.

In the measurement of angular velocity of the brushless motor, the rpm setting value on a spin coater is determined which starts from 4000 to 18,000 rpm. The brushless motor only produces the minimum angular velocity of 4000 rpm and the maximum angular velocity of 16,637 rpm under no-load conditions. From data, the created spin coater has an accuracy rate of 98.9%. The results can be seen in **Figure 27** and **Table 3**.

http://dx.doi.org/10.5772/66815

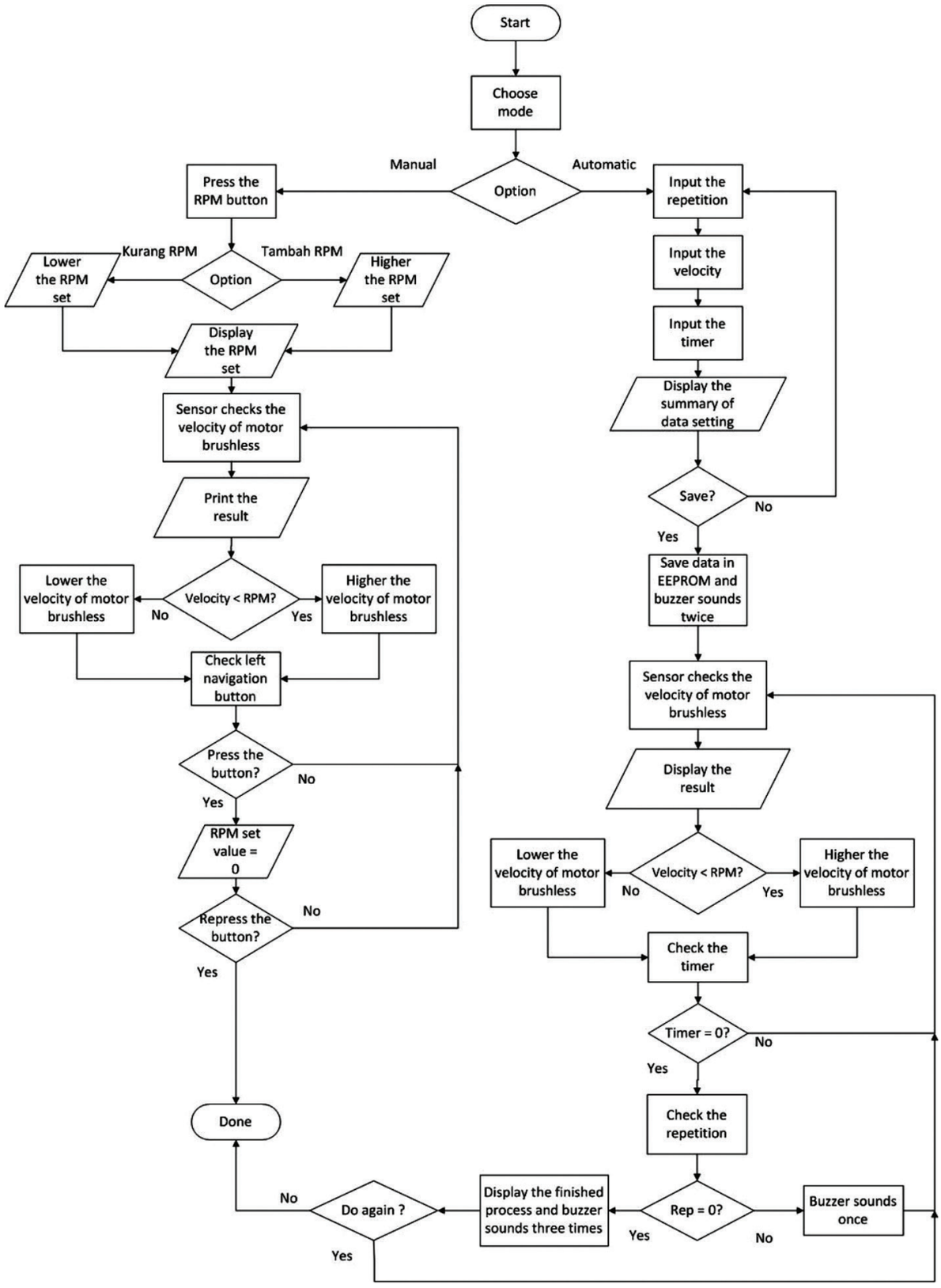

Figure 15. Program flowchart of a spin coater in the automatic mode.

Figure 16. Display of mode select.

Figure 17. Display of repetition setting.

Figure 18. Display of velocity setting.

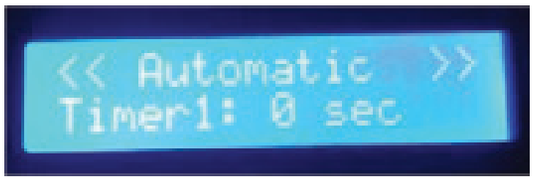

Figure 19. Display of time setting.

Figure 20. Display of setting summary.

Figure 21. Display of set saving.

http://dx.doi.org/10.5772/66815

Figure 22. Display of data saving.

Figure 23. Display of saved data.

Figure 24. Display of the spin coating process.

Figure 25. Display of the finished process.

Figure 26. Display of the spin coating reprocess.

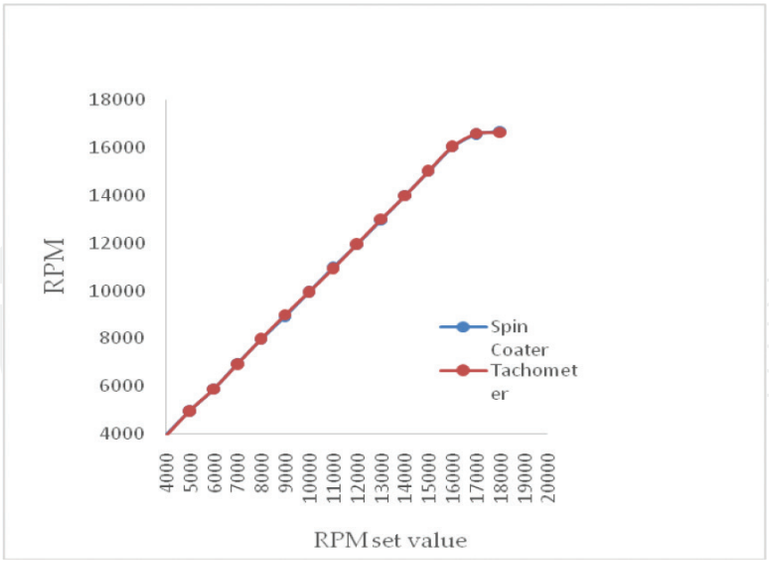

Figure 27. Comparison results of angular velocity after development.

Testing the angular velocity (RPM)			Accuracy level of spin coater (%)
Set value	**Spin coater**	**Tachometer**	
4000	3960	3916	99
5000	4980	4977	99.6
6000	5880	5887	98
7000	6960	6938	99.42
8000	7980	7998	99.75
9000	8940	9002	99.33
10,000	9960	9966	99.6
11,000	10,980	10,932	99.82
12,000	11,940	11,960	99.5
13,000	12,960	12,996	99.69
14,000	13,980	13,974	99.86
15,000	15,000	15,027	100
16,000	16,020	16,046	99.86
17,000	16,560	16,587	97.41
18,000	16,680	16,637	92.67
Mean			98.9

Table 3. Comparison data of angular velocity after development.

http://dx.doi.org/10.5772/66815

4. Results and applications

This method has been developed in our laboratory to fabricate thin films, especially ferroelectric thin films such as barium strontium titanate (BST), lithium tantalate ($LiTaO_3$), lithium niobate ($LiNbO_3$), and copper oxide (CuO) thin films. Specifically for BST ferroelectric thin films, its patent has been registered in Indonesia with a number of P00201201119 in 2013.

BST thin films of the modified spin coating method resulting in a dielectric constant of 2–18 and conductivity values of 1.6×10^{-6} to 2.4×10^{-9} S/cm at the voltages of 1–4 V [34]. In addition, the particle distribution size of BST 0.45 is 134.93 nm which is smaller than BST 0.25 which gives 186.26 nm, BST 0.35 gives a value of 467.86 nm, and BST 0.55 is 407.49 nm [34].

BST thin films have been developed in a number of applications such as temperature and light sensors that are applied into the automatic drying system [35], light sensors into the luxmeter system [36] and sensors in the blood sugar level system, its patent has been registered in Indonesia with a number of P00201508327 in 2015.

In the automatic drying system [35], light sensors have 0.176 mV/lux, which is the best sensitivity. While the best temperature sensor has a value range of 30–109°C, a sensitivity of 0.862 mV/°C, a film resolution of 1°C, an accuracy level of 92.2%, and small hysteresis [35]. These sensors, which are then integrated into microcontroller, have been successfully conducted on an ATMega8535 microcontroller based on our automatized drying system model.

In the luxmeter system [36], $Ba_{0,25}Sr_{0,75}TiO_3$ (BST) thin films have been deposited on a Si (100) p-type substrate by a chemical solution deposition (CSD) method followed by the spin coating technique (at 3000 rpm rotational speed for 30 seconds). This BST has an electrical conductivity of 2.79×10^{-7} to 5.3×10^{-7} S/cm, which are in the range of semiconductor materials. The *I-V* measurement on the films which was carried out under dark and bright conditions results in convincing conclusion that the films are photodiodes. The maximum optical absorbance found for green light with a wavelength of around 550 nm.

The blood sugar level system also uses the modified spin coating method. The test results showed that the light intensity that was received by photodiode sensor, represented by the output voltage, will change in line with changes in the value of blood sugar levels, follows the equation $y = 0.0014x^2 - 0.6652x + 139.34$. The coefficient of $R^2 = 0.9544$ indicates that x has a major effect on y, so that it can be concluded that the photodiode sensor can work well as a sensor of blood sugar level instrument. Accuracy and precision of the instrument are 98.92 and 97.41%, respectively.

BST thin films as solar cells enhanced by photonic crystals are currently being developed [37]. This enhancement needs higher angular velocity (>6000 rpm) than previous works in BST (3000 rpm). The second generation of modified spin coater is used for coating the thin films to fulfill the requirement. The optical characterization of BST ($Ba_xSr_{1-x}TiO_3$) using a photonic crystal resulted in the average absorption percentages for mole fraction x = 0.25, 0.35, 0.45,

and 0.55 were 92.04, 83.55, 91.16, and 80.12%, respectively [37]. In addition, the BST thin film with the embedded photonic crystal exhibited a relatively significant enhancement on photon absorption, with increasing values of 3.96, 7.07, 3.04, and 13.33%, respectively.

Furthermore, BST thin films are worked both as sensors and solar cells can be applied to the more sophisticated fields such as temperature and light sensors in the satellite technology [38, 39], photodiode in satellite technology [40], as well as solar cells for substituting conventional battery in satellite technology [41].

$LiTaO_3$ thin films have also been developed by using the modified spin coating method as infrared sensors that are expected to be developed as an automatic switch in satellite technology [42]. These thin films have electrical conductivities of 10^{-6}–10^{-5} S/cm and the diffusion coefficient values of 57–391 nm^2/s [43] as well as the energy gaps of 3.41–4.56 eV [42] while the $LiTaO_3$ thin films have energy gaps of 2.43–2.80 eV [44]. The $LiNbO_3$ thin films that were enhanced by a lanthanum dopant also use a velocity of 3000 rpm and have the energy gaps of 2.43–2.80 eV [45].

In addition to BST, $LiTaO_3$, and $LiNbO_3$, we are also develop other thin films, i.e., CuO thin films. This film is also developed as solar cells. CuO thin films were enhanced by photonic crystals that have absorbance in the visible region and energy gaps of 1.89–2.05 eV [46].

5. Conclusion

The modified spin coaters both first and second generation have given very good results on ferroelectric films, which are BST, $LiTaO_3$, $LiNbO_3$, and CuO, as sensors and solar cells. In BST, the modified spin coater enhances the photon absorption percentages by using photonic crystals which need higher angular velocity (6000 rpm). Another ferroelectric thin film that use 3000 rpm also have given good results in energy gap, electrical conductivity, etc. From these data, they were succeed to be applied in an instrument or a device such as a blood sugar level, automatic drying, and luxmeter systems. In addition, these thin films also have potential to be applied in more sophisticated fields such as photodiode in satellite technology, temperature, and light sensors in the satellite technology, as well as solar cells for substituting conventional battery in satellite technology.

Acknowledgements

This work was funded by Grant of International Research Collaboration and Scientific Publication from Ministry of Research, Technology and Higher Education, Republic of Indonesia under contract No. 082/SP2H/UPL/DIT.LITABMAS/II/2015 and Hibah Penelitian Institusi, Ministry of Research, Technology and Higher Education, Republic of Indonesia under contract No. 079/SP2H/LT/DRPM/II/2016.

Author details

Irzaman[1]*, Heriyanto Syafutra[1], Ridwan Siskandar[2], Aminullah[3] and Husin Alatas[1]

*Address all correspondence to: irzaman@apps.ipb.ac.id

1 Department of Physics, Faculty of Mathematics and Natural Sciences, Bogor Agricultural University, Bogor, Indonesia

2 Bogor Agricultural University, Bogor, Indonesia

3 Department of Food Technology and Nutrition, Djuanda University, Bogor, Indonesia

References

[1] Hamdani A, Komaro M, Irzaman. Development of Solar Cell based on Ferroelectric $LiTaO_3$ using Spin Coating Method for Green Electric Power, Scientific Report of Indonesia Institute of Science 2009 pp. 7. (in Indonesia)

[2] Lee JS, Park JS, Kim JS, Lee JH, Lee YH, Hahn SR. Preparation of BST Thin Films with High Pyroelectric Coefficients an Ambient Temperatures. Jpn. J. Appl. 1999**. 38**(5B), L574.

[3] Irzaman, Darmasetiawan H, Hardhienata H, Erviansyah R, Akhiruddin, Hikam M, Arifin P. Electrical Properties of Photodiode BST Thin Film Doped with Ferrium Oxide using Chemical Deposition Solution Method. J. At. Indonesia, Batan. 2010. **6**(2), 57–62. (in Indonesia).

[4] Irzaman, Syafutra H, Darmasetiawan H, Hardhienata H, Erviansyah R, Huriawati F, Akhiruddin, Hikam M, Arifin P. Electrical Properties of Photodiode $Ba_{0.25}Sr_{0.75}TiO_3$ (BST) Thin Film Doped with Ferric Oxide on p-type Si (100) Substrate using Chemical Solution Deposition Method. At. Indonesia. 2011. **37**(3), 133–138. (in Indonesia).

[5] I. Novianty, S. Yani, R. Chahyani, Z. Athiyah, Casnan, Fendi, S. Serah, J. Hartono, N. Rofiah, H. Syahfutra, Akhiruddin and Irzaman. Electrical Properties $Fe2o_3$ Doped Based $Ba_{0.25}Sr_{0.75}TiO_3$. Thin Film As Light Sensor. Jurnal SainsMateri Indonesia. 2011 Vol. Materials for Sensor Special Edition, pp. 9–12.

[6] Irzaman, Syafutra H, Rancasa E, Nuayi AW, Rahman TGN, Nuzulia NA, Supu I, Sugianto, Tumimomor F, Surianty, Muzikarno O, Masrur. The Effect of Ba/Sr ratio on Electrical and Optical Properties of $Ba_xSr_{(1-x)}TiO_3$ (x = 0.25; 0.35; 0.45; 0.55) Thin Film Semiconductor. Ferroelectrics. 2013. **445**(1), 4–17.

[7] Baumert BA, Chang LH, Matsuda AT, Tracy CJ. A Study of BST Thin Films for Use in bypass Capacitors. J. Mater. 1998. **13(**1), 197.

[8] Itskovsky MA. Kinetics of Ferroelectric Phase Transition: Nonlinear Pyroelectric Effect and Ferroelectric Solar Cell. Jpn. J. Appl. Phys. 1999. **38**(8), 4812.

[9] Darmasetiawan H, Irzaman, Indro MN, Sukaryo SG, Hikam M, Bo NP. Optical Properties of Crystalline Ta_2O_5 Thin Films. Phys. Stat. Sol. (a), Germany. 2002. **193**, 53–60.

[10] Irzaman, Darvina Y, Fuad A, Arifin P, Budiman M, Barmawi M. Physical and Pyroelectric Properties of Tantalum Oxide Doped Lead Zirconium Titanate [$Pb_{0.9950}(Zr_{0.525}Ti_{0.465}Ta_{0.010})O_3$] Thin Films and Its Application for IR Sensor. Phys. Stat. Sol. (a), Germany. 2003. **199,** 416–424.

[11] Irzaman, Darmasetiawan H, Hikam M, Arifin P, Budiman M, Barmawi M. Pyroelectric Properties of Lead Zirconium Titanate ($PbZr_{0.525}Ti_{0.475}O_3$) Metal-Ferroelectric-Metal Capacitor and Its Application for IR Sensor. In: International Conference on Materials for Advances Technology (ICMAT), Materials Research Society, Singapore. 2003. pp. 7–12.

[12] Dahrul M, Syafutra H, Arif A, Irzaman, Indro, Siswadi MN. Synthesis and Characterizations Photodiode Thin Film Barium Strontium Titanate (BST) Doped Niobium and Iron as Light Sensor. In: The 4th Asian Physics Symposium, American Institute of Physics (AIP) Conference. 2010. **1325**, pp. 43–46.

[13] Hikam M, Sarwono E, Irzaman. Calculation on Spontaneous Polarization and Electric Quadrupole Moment of PIZT (PbInxZryTi1-x-yO3-x/2) Material. Makara, Sains. 2004. **8**, 108–115. (in Indonesia)

[14] Irzaman, Maddu A, Syafutra H, Ismangil A. Test on Electrical Conductivity and Dielectric of Lithium Tantalite ($LiTaO_3$) Doped by (Nb_2O_5) using Chemical Deposition Method. In: Proceedings of National Workshop on Physics. 2010. pp. 175–183. (in Indonesia)

[15] Umiati NAK, Irzaman, Budiman M, Barmawi M. Annelaing Effect on the Growth of $PbZr_{0.625}Ti_{0.375}O_3$ (PZT). Thin Film. Kontribusi Fisika Indonesia. 2001. **12**, 94–98 (in Indonesia).

[16] Choi ES, Lee JC, Hwang JS, Yoon SG. Electrical Characteristics of The Contour Vibration Mode Piezoelectric Transformer with Ring/Dot Electrode Area Ratio. Jpn. J. Appl. Phys. 1999. **38**(9B), 5317.

[17] Momose S, Nakamura T, Tachibana K. Effects of Gas Phase Thermal Decompositions of Chemical Vapor Deposition Source Molecules on The Deposition of BST Films. Jpn. J. Appl. Phys. 2000. **39**, (9B), 5384.

[18] Gao Y, He S, Alluri P, Engelhard M, Lea AS, Finder J, Melnick B, Hance RL. Effect of Precusors and Substrate Materials on Microstructure, Dielectric Properties and Step Coveage of (Ba, Sr)TiO_3 Films Grown by Metalorgic Chemical Vapor Deposition. J. Appl. Phys. 2000. **87**, 124–132.

[19] Auciello O, Scott JF, Ramesh R. The Physics of Ferroelectric Memories. Am. Inst. Phys. 1998. **51**, 22–27.

[20] Verma K, Sharma S, Sharma DK, Kumar R, Rai R. Sol-gel Processing and Characterization of Nanometersized (Ba,Sr)TiO_3 Ceramics. Adv. Mater. Lett. 2012. **3**(1), 44–49.

[21] Giridharan NV, Jayavel R, Ramasamy P. Structural, Morphological and Electrical Studies on Barium Strontium Titanate Thin Films Prepared by Sol-Gel Technique. Chennai: Crystal Growth Centre, Anna University; 2001.

[22] Chen X, Cai W, Fu C, Chen H, Zhang Q. Synthesis and Morphology of $Ba(Zr_{0.20}Ti_{0.80})O_3$ Powder Obtained by Sol-Gel Method. J. Sol-Gel Sci. Technol. 2011. **57**, 149–156.

[23] Wang F, Uusimaki A, Leppavuori S, Karmanenko SF, Dedyk AI, Sakharov VI, Serenkov IT. BST Ferroelectric Film Prepared with Sol-Gel Process and Its Dielectric Performance in Planar Capacitor Structure. J. Mater. Res. 1998. **13**(5), 1243.

[24] Tyunina M. Dielectric Properties of Atomic Layer Deposited Thin Film Barium Strontium Titanate. Integr. Ferroelectr. 2008. **102**, 29–36.

[25] Suherman PM. Comparison of Structural Microstructural and Electrical Analyses of Barium Strontium Titanate Thin Films. J Appl. Phys. 2009. **105**, 1–6.

[26] Kim S, Kang TS, Je JH. Structural Characterization of Laser Alblation Epitaxial BST Thin Films on MgO (001) by Synchrotron X-Ray Scattering. J. Mater. 1999. **14**(7), 2905.

[27] Zhu XH, Zheng DN, Peng JL, Chen YF. Enhanced Dielectic Properties of Mn Doped $Ba_{0.6}Sr_{0.4}TiO_3$ Thin Films Fabricated by Pulsed Laser Deposition. Mater. Lett. 2005. **60,** 1224–1228.

[28] Izuha M, Ade K, Koike M, Takeno S, Fukushima N. Electrical Properties and Microstructure of Pt/BST/$SrRuO_3$ Capacitors. Appl. Phys. Lett. 1997. **70**(11), 1405.

[29] Purwanto R, Prajitno G. Speed and Rotation Time Variation in TiO_2 Coating Process for the Development of DSSC made from Garcinia Mangostana Extract as Dye Sensitizer. Jurnal Sains dan Seni POMITS. 2013. **2**(1), 2337–3520 (in Indonesia).

[30] Hikam M, Irzaman, Darmasetiawan H, Yogaraksa T. Study on Crystaline of PbZrxTi1-xO3 made by Spin Coating method. J. Sains Mater. Indonesia. 2002. **4**(1), 16–19. (in Indonesia).

[31] Rahmawati E, Robiandi F, Didik LA, Rahayu S, Santjojo DJDH, Sakti SP, Masruroh. Effect of Xylene and Tetrahydrofuran on the Thickness of Polystyrene using Spin Coating Method. Natural. 2014. **2**(4), 1–6. (in Indonesia).

[32] Herrera MA, Mathew AP, Oksman K. Gas Permeability and Selectivity of Cellulose Nanocrystals Films (layers) Deposited by Spin Coating. Carbohydrate Polym. 2014. **112,** 494—501.

[33] Manikandan N, Shanti B, Muruganand S. Construction of Spin Coating Machine Controlled by Arm Processor for Physical Studies of PVA. Int. J. Electron. Electr. Eng. 2015. **3**(4), 1–5.

[34] Irzaman, Syafutra H, Arif A, Alatas H, Hilaluddin MN, Kurniawan A, Iskandar J, Dahrul M, Ismangil A, Yosman D, Aminullah, Prasetyo LB, Yusuf A, Kadri TM. Formation of Solar. Cells Based On $Ba_{0.5}Sr_{0.5}TiO_3$ (BST) Ferroelectric Thick Film. AIP Proceeding, USA, **1586**. 2014. 24–34.

[35] Irzaman, Siskandar R, Aminullah, Irmansyah, Alatas H. Characterization of $Ba_{0.55}Sr_{0.45}TiO_3$ Films As Light and Temperature Sensors And Its Implementation on Automatic Drying System Model. Integr. Ferroelectr. 2016. **168** (1), 130–150.

[36] Syafutra H, Irzaman, Indro MN, Subrata IDM. Development of Luxmeter Based on $Ba_{0.25}Sr_{0.75}TiO_3$ Ferroelectric Material. AIP Conf. Proc. 2010. **1325**, 75.

[37] Abd. Wahidin Nuayi, H. Alatas, Irzaman, and M. Rahmat. Enhancement of Photon Absorption on $Ba_xSr_{1-x}TiO_3$ Thin-Film Semiconductor Using Photonic Crystal. Hindawi. 2014. 2014, 1–8.

[38] Kurniawan A, Yosman, Arif A, Juansah J, Irzaman. Development and Application of $Ba_{0.5}Sr_{0.5}TiO_3$ (BST) Thin Film as Temperature Sensor for Satellite Technology. Procedia Environ. Sci. 2015. **24,** 335–339.

[39] Iskandar J, Syafutra H, Juansah J, Irzaman. Characterizations of Electrical and Optical Properties on Ferroelectric Photodiode of Barium Strontium Titanate ($Ba_{0.5}Sr_{0.5}TiO_3$) Films Based on the Annealing Time Differences and Its Development as Light Sensor on Satellite Technology. Procedia Environ. Sci. 2015. **24,** 324–328.

[40] Setiawan A, Aminullah, Juansah J, Irzaman. Optical and Electrical Characterizations of Niobium-doped $Ba_{0.25}Sr_{0.75}TiO_3$ (BSNT) on p-type Silicon and Corning Glass Substrates and Its Implementation as Photodiode on Satellite of LAPAN-IPB. Procedia Environ. Sci. 2016. **33,** 620–625.

[41] Irzaman, Putra IR, Aminullah, Syafutra H, Alatas H. Development of Ferroelectric Solar Cells of Barium Strontium Titanate ($Ba_xSr_{1-x}TiO_3$) for Subtituting Conventional Battery in LAPAN-IPB Satellite (LISAT). Procedia Environ. Sci. 2016. **33,** 607–614.

[42] Ismangil A, Jenie RP, Irmansyah, Irzaman. Development of Lithium Tantallite ($LiTaO_3$) for Automatic Switch on LAPAN-IPB Satellite Infra-red Sensor. Procedia Environ. Sci. 2015. **24,** 329–334.

[43] Ismangil A, Irmansyah, Irzaman. The Diffusion Coefficient of Lithium Tantalite ($LiTaO_3$) with Temperature Variations on LAPAN-IPB Satellite Infra-red Sensor. Procedia Environ. Sci. 2016. **33,** 668–673.

[44] Irzaman, Pebriyanto Y, Rosidah E, Apipah, Noor I, Alkadri A. Characterization of Optical and Structural of Lanthanum Doped $LiTaO_3$ Thin Films. Integrated Ferroelectr. 2015. **167**(1), 137–145.

[45] Irzaman, Sitompul H, Masitoh, Misbakhusshudur M, Mursyidah. Optical and Structural Properties of Lanthanum Doped Lithium Niobate Thin Films. Ferroelectrics. 2016. **502**, 9–18.

[46] Dahrul M, Alatas H, Irzaman. Preparation and Optical Properties Study of CuO Thin Film as Applied Solar Cell on LAPAN-IPB Satellite. Procedia Environ. Sci. 2016. **33,** 661–667.